

# Derivation of the Disorder Induced Interaction and the Phase Diagram of Cuprate Superconductors

E. V. L. DE MELLO, AND RAPHAEL B. KASAL

<sup>1</sup> *Instituto de Física, Universidade Federal Fluminense, Niterói, RJ 24210-340, Brazil*

PACS 74.20.-z – Theories and Models of Superconducting State

PACS 74.25.Dw – Superconductivity Phase Diagram

PACS 74.72.-h – Cuprate Superconductors

**Abstract.** - We show that an electronic phase transition described by the Cahn-Hilliard equation has important applications to cuprate superconductors. The simulations of the local charge density and free energy reveal two main features: i) The segregation process creates tiny isolated regions with potential wells where the holes can be bound in single-particle levels. ii) The clustering process also gives rise to an effective two-body pairing interactions and superconducting amplitudes  $\Delta_{sc}(\vec{r})$  at low temperatures. The resulting system resembles a granular superconductor with the resistivity transition driven by Josephson coupling among these nanoscale grains. This approach reproduces the well known critical temperature transition  $T_c(p)$  as function of the doping level  $p$ . Furthermore, the local density of states with spatial dependent gaps  $\Delta(\vec{r})$  is due to the intragrain single-particle bound states that remain above  $T_c$ , which characterizes the pseudogap phase and reproduces many measurements.

**Introduction.** – The origin of the superconducting gap associated with the superconducting state and the relation to the pseudogap above the transition temperature ( $T_c$ ) remains one of the central questions in high- $T_c$  research [1–3]. It is a matter of debate whether this problem is connected with the charge inhomogeneities observed in many experiments [4–6] and with the position dependent energy gap  $\Delta(\vec{r})$  measured by Scanning Tunneling Microscopy (STM) [7–13]. In this letter we suggest that these two problems are strongly related and their solution must be worked out together.

There are steadily accumulating evidences that the charge distribution is microscopically inhomogeneous in the  $CuO_2$  planes of high temperature superconductors (HTSC). The most well known charge inhomogeneity is the charge stripe structure [4, 5] Nuclear quadrupole resonance (NQR) have measured two signals corresponding to two (low and high) densities around the average doping [6], that increases as the temperature is decreased. This evolution with temperature can be an evidence of an electronic phase separation (EPS). More recently, NQR experiments indicated that the charge inhomogeneity in the planes is correlated with the  $O$  dopant atoms in the  $YBa_2Cu_3O_y$  system [14]. Similarly, recent STM data have revealed one of the most puzzling property of cuprates, the non-uniform

energy gaps  $\Delta(\vec{r})$  on the length scale of nanometers [7–13]. The derived LDOS have generally two forms: one type with smaller gaps and well defined peaks and other with larger gaps and ill-defined peaks [8]. Furthermore, some of these gaps remain well above the superconducting critical temperature  $T_c(p)$  [9, 10]. These two types of gaps [3] may occur due to the existence of two energy scales that have been observed on electronic Raman scattering measurements [15], STM data [11–13], Angle Resolved Photon Emission (ARPES) [16] and combined STM-ARPES [17]. However, the origin and even the existence of this two-gap picture is still a matter of debate [18, 19].

In order to obtain an unified interpretation to all of these experiments we study an EPS transition that generates regions of low and high densities. Such transition may be driven by the lower free energy of undoped antiferromagnetic (AF) regions [20] (intrinsic) or by the out of plane dopants [14] (extrinsic origin). As  $p$  increases, the Coulomb repulsion among the charges in the local high doping regions increases the energy cost of the phase separation, which ceases the transition in the overdoped region, in agreement with the disappearance of the local AF fluctuations [21]. This clustering phenomenon gives rise to a potential that bunch up the holes and separates low and high density phases in the form of small domains or

grains in the  $CuO_2$  planes. This EPS process can be regarded as due to an effective attractive potential, which is used in the self-consistent calculations to obtain the intra-grain superconducting amplitudes. In this approach the resistivity transition temperature  $T_c(p)$  occurs when the Josephson energy  $E_J(p)$  among the separated regions is equal to  $K_B T_c(p)$ .

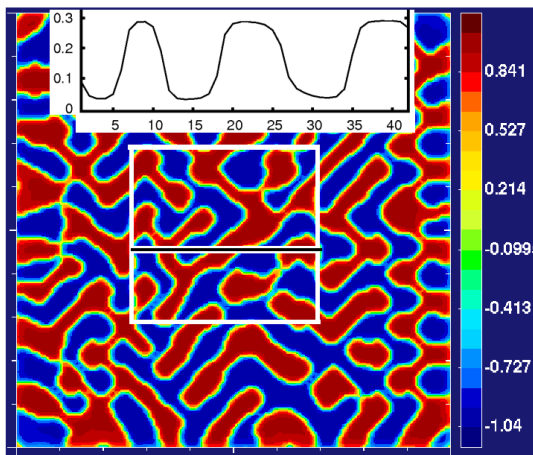


Fig. 1: (color online) The density map simulation of the inhomogeneous charge density on a grid with  $105 \times 105$  sites. The white square indicates where the superconducting calculations are made. For the  $p = 0.16$  compound, the local densities  $p_i$  along the line with a black trace are shown on the top of the figure.

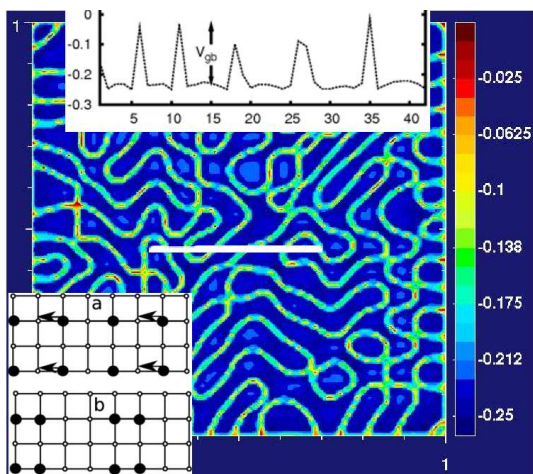


Fig. 2: (color online) The simulation of the potential  $V(p, i, T)$ . The values on 42 sites at the white line are shown in the top inset to demonstrate the potential wells with average barrier  $\approx V_{gb}$  where single-particle bound states are formed. The low inset shows schematically an example of the  $V(p, i, T)$  minimization with the holes (black dots) clustering by the CH diffusion as an effective two-body hole attraction.

### The Potential from the Charge Inhomogeneities.

Phase separation is a very general phenomenon in which a structurally and chemically homogeneous system shows instability toward a disordered composition [22]. As discussed above, it has been recognized to be very important to cuprate superconductors [23] but there is not a theory to describe the degree of disorder as function of doping and temperature. Consequently, to deal with this problem, we use the general theory of Cahn-Hilliard (CH) [24–26] adapted to the cuprates. The starting point is the EPS temperature  $T_{PS}(p)$ , taken close to the upper pseudogap that produces an anomaly measured in some experiments [1–3]. The transition order parameter is the difference between the local and the average charge density  $u(p, i, T) \equiv (p(i, T) - p)/p$ . Clearly  $u(p, i, T) = 0$  corresponds to the homogeneous system above  $T_{PS}(p)$ . Then the typical Ginzburg-Landau free energy functional in terms of  $u(p, i, T)$  is given by

$$f(u) = \frac{1}{2}\varepsilon^2|\nabla u|^2 + V(u, T). \quad (1)$$

Where the potential  $V(u, T) = -A^2(T)u^2/2 + B^2u^4/4 + \dots$ ,  $A^2(T) = \alpha(T_{PS}(p) - T)$ ,  $\alpha$  and  $B$  are constants.  $\varepsilon$  gives the size of the boundaries between the low and high density phases [25,26]. The CH equation can be written [22] in the form of a continuity equation of the local density of free energy  $f$ ,  $\partial_t u = -\nabla \cdot \mathbf{J}$ , with the current  $\mathbf{J} = M\nabla(\delta f/\delta u)$ , where  $M$  is the mobility or the charge transport coefficient that sets the time scale. Therefore,

$$\frac{\partial u}{\partial t} = -M\nabla^2(\varepsilon^2\nabla^2 u - A^2(T)u + B^2u^3). \quad (2)$$

In Fig.(1), we show a typical simulation of the density map with the two (hole-rich and hole-poor) phases given by different colors.

The potential  $V(p, i, T)$  isolates the hole-rich and hole-poor regions forming grain boundaries between these two phases [26].  $V(p, i, T)$  reaches its minimum value at the low and high equilibrium densities as it is demonstrated by the simulations shown in Fig.(1) and Fig.(2). Our most important finding is that  $V(p, i, T)$  produces two different effects: first, it creates potential wells as it is shown in the top inset by the values of  $V(p, i, T)$  on 42 sites along the white straight line. The potential barriers among the grains can be approximated by  $V_{gb}(p, T)$  and confines the holes, generating local or intragrain single-particle bound states. The signature of these single-particle bound states will appear in the local density of states together with the superconducting gap from the two-body attraction. Second, and more important, *to minimize the local free energy, the holes move to equilibrium positions in a similar fashion as if they attract themselves*. This is schematically illustrated in the low inset of Fig.(2) where a) represents a homogeneous system with  $p = 0.25$  (one hole at each four sites) and b) the motion toward clusters formation of low ( $p_i = 0$ ) and high densities ( $p_i = 0.50$ ), according

to the CH diffusion process. Clearly, this movement of holes can be regarded as originated from *an effective two-body attraction*, like the spin-spin exchange interaction, that arises from the Pauli principle and the electrons wave functions. We do not know the exact strength of this potential but it should scale with the potential barrier  $V_{gb}(p, T)$  between the two phases. We discuss below that this effective potential can give rise to superconducting pairs.

**The Self-consistent Calculations.** – The calculated  $u(i, T)$  (or  $p(\mathbf{x}_i, T)$ ) on square lattices like the  $42 \times 42$  shown in Fig.(1) is used as the *initial input* and *it is maintained fixed* throughout the self-consistent Bogoliubov-deGennes (BdG) calculations. The pairing potential  $V_{gb}(p, T)$  is adjusted to match the average local density of states (LDOS) measured by low temperature STM on  $0.11 \leq p \leq 0.19$  Bi2212 compounds [8], namely,  $V_{gb}(p, T = 0) = (0.7 - 2.36 \times p)$  (eV). Starting with an extended Hubbard Hamiltonian, the BdG equations are [20, 26–30].

$$\begin{pmatrix} K & \Delta \\ \Delta^* & -K^* \end{pmatrix} \begin{pmatrix} u_n(\mathbf{x}_i) \\ v_n(\mathbf{x}_i) \end{pmatrix} = E_n \begin{pmatrix} u_n(\mathbf{x}_i) \\ v_n(\mathbf{x}_i) \end{pmatrix} \quad (3)$$

These equations, defined in detail in Refs. [26–30], are solved self-consistently.  $u_n, v_n$  and  $E_n \geq 0$  are respectively the eigenvectors and eigenvalues. As mentioned, the hole clustering process is mainly along the  $Cu - O$  bonds, and with the Coulomb repulsion, it favours the d-wave pairing. Thus, the d-wave pairing amplitudes are given by

$$\begin{aligned} \Delta_d(\mathbf{x}_i) = & -\frac{V_{gb}}{2} \sum_n [u_n(\mathbf{x}_i)v_n^*(\mathbf{x}_i + \delta) + v_n^*(\mathbf{x}_i)u_n(\mathbf{x}_i \\ & + \delta)] \tanh \frac{E_n}{2k_B T}, \end{aligned} \quad (4)$$

and the inhomogeneous hole density is given by

$$p(\mathbf{x}_i) = 1 - 2 \sum_n [|u_n(\mathbf{x}_i)|^2 f_n + |v_n(\mathbf{x}_i)|^2 (1 - f_n)], \quad (5)$$

where  $f_n$  is the Fermi function. We stop the self-consistent calculations only when all  $p(\mathbf{x}_i)$  converges to the CH density map shown in Fig.(1).

Due to the  $Cu$  d-orbitals and the strong on site Coulomb repulsion, we calculate only the intra-grain d-wave superconducting gap  $\Delta_d(i, T)$ . The effect of the temperature in the potential is taken into account by  $V_{gb}(T) \sim (1 - (T/T_{PS})^{1.5})$ , as demonstrated by CH [24] near  $T_{PS}$ , and consequently,  $\Delta_d(i, T) \rightarrow 0$  at a single temperature  $T^*(p)$ . The fact that all gaps vanishes at the same temperature although the values of  $\Delta_d(i, T = 0)$  can be very different is a consequence of the self-consistent mean field approach.

As the top inset of Fig.(2) shows, the different local densities regions are bounded by the potential barriers  $\approx$

$V_{gb}$ . As the temperature goes down, the barriers increases forming an metal-insulator-metal junction. Consequently, the electronic structure in the  $CuO - 2$  planes becomes similar to that of a granular superconductor [31]. In this way the superconducting transition occurs in two steps: first by the appearing of intra-grain superconductivity in the grains and than by Josephson coupling with phase locking among all the hole-rich and hole-poor regions at a lower temperature.

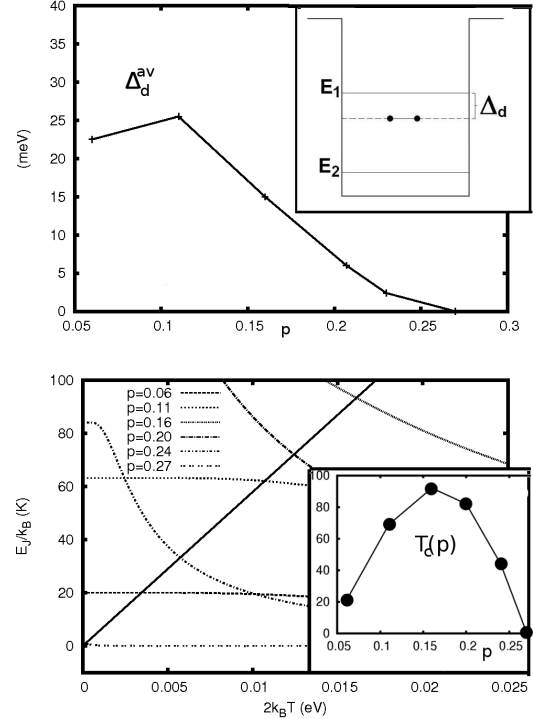


Fig. 3: Top panel, the average  $\Delta_d(p)$ , and in the inset, the schematic single particle and superconducting energy levels present in each nanoscopic grain. In the low panel, the thermal energy  $k_B T$  and the Josephson coupling among superconducting grains  $E_J(p, T)$  for some selected doping values as function of  $T$ . The intersections give  $T_c(p)$ , as plotted in the inset.

By using the theory of granular superconductors [32] to these electronic grains and the calculated average superconducting amplitudes  $\Delta_d^{av}(T, p) \equiv \sum_i^N \Delta_d(T, i, p)/N$ , where  $N$  is the total number of sites, we can estimate the values of  $T_c(p)$ .

$$E_J(p, T) = \frac{\pi \hbar \Delta_d^{av}(T, p)}{4e^2 R_n} \tanh\left(\frac{\Delta_d^{av}(T, p)}{2K_B T_c}\right). \quad (6)$$

Where  $\Delta_d^{av}(T, p)$  is the average of the local superconducting gaps  $\Delta_d(i, p, T)$  on a  $N \times N$  ( $N = 28, 36$  and  $42$ ) square lattice which is plotted in the top panel of Fig.(3). The inset shows the schematically single particle levels at a shallow puddle whose walls are proportional to  $V_{gb}$ .  $R_n$  is the normal resistance of a given compound, which is

proportional to the planar resistivity  $\rho_{ab}$  measurements [33] on the  $La_{2-p}Sr_pCuO_2$  series.

In the low panel of Fig.(3), the Josephson coupling  $E_J(p, T)$  is plotted together with the thermal energy  $k_B T$  whose intersection yields the critical temperature  $T_c(p)$ , as shown in the inset. The fact that  $T_c(p)$  has the well known dome shape is due to the different behavior of  $\Delta_d^{av}(T, p)$  that decreases with  $p$  (Fig.(3)) and  $1/R_n$  that increases with  $p$ . The values are in reasonable agreement with the Bi2212  $T_c(p)$ , as expected, since  $V_{gb}$  was chosen to match the Bi2212 low temperature LDOS gaps [8]. Since, in general  $T^*(p) > T_c(p)$ , this approach provides an interpretation to the superconducting amplitude and the measured quasiparticles dispersion in the normal phase [18, 19].

**The LDOS and superconducting gap.** – In the BdG approach, the symmetric local density of states (LDOS) is proportional to the spectral function [34] and may be written as

$$N_i(T, V_{gb}, eV) = \sum_n [|u_n(\mathbf{x}_i)|^2 + |v_n(\mathbf{x}_i)|^2] \times [f'_n(eV - E_n) + f'_n(eV + E_n)]. \quad (7)$$

The prime is the derivative with respect to the argument.  $u_n, v_n$  and  $E_n$  are respectively the eigenvectors and eigenvalues of the BdG matrix equation [26, 27],  $f_n$  is the Fermi function and  $V$  is the applied voltage.  $N_i(T, V_{gb}, eV) \equiv LDOS(V_{gb})$  is proportional to the tunneling conductance  $dI/dV$ , and we probe the effects of the inhomogeneous potential by examining the ratio  $LDOS(V_{gb} \neq 0)/LDOS(V_{gb} = 0)$ . This LDOS ratio yields well-defined peaks and converges to the unity at large bias, similar LDOS ratios calculated from STM measurements [9, 10].

These features are illustrated in Fig.(4) for a representative overdoped  $p = 0.20$  compound near a grain boundary at a representative average doping hole point. At  $T = 40K$ ,  $V_{gb} = 0.240eV$  and for large applied potential difference ( $V > 0.1eV$ ) both LDOS,  $LDOS(V_{gb} \neq 0)$  and  $LDOS(V_{gb} = 0)$  converge to the same values. An important result of our calculations is that the LDOS yield peaks at larger bias than the values of the superconducting amplitude  $\Delta_d(i, p, T)$ . In Fig.(4) we can see the LDOS gap  $\Delta_{PG} = 24meV$  (Eq.(7) and the much smaller superconducting gap  $\Delta_d = 7.2meV$  (Eq.(4)) that is almost undiscernable and therefore it is marked by arrows. We attribute  $\Delta_{PG}$  to the single-particle bound states in the grains. In our calculations we can see that hole-poor produces larger and not well defined peaks than those at hole-rich regions as noticed by McElroy et al [8]. The physical explanation is that, if the number of holes in a grain is large (hole-rich grain) they occupy higher single-particle levels in the local potential wells and can be more easily removed by the STM tip.

To study the pseudogap phase we perform calculations on an underdoped compound with  $p = 0.11$  and  $T_c \approx 65K$  according Fig.(3). In Fig.(5) we show the results at

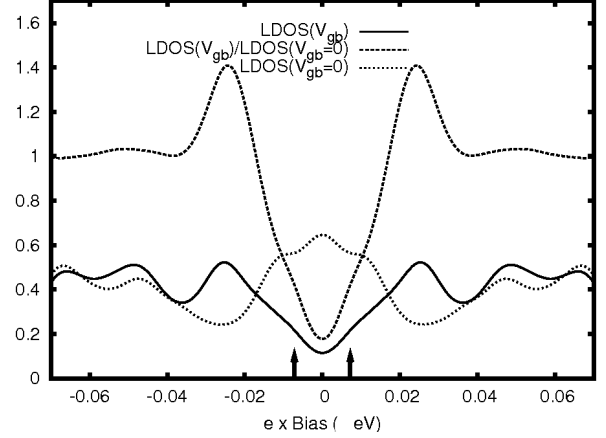


Fig. 4: The LDOS on an overdoped  $p = 0.20$  sample for  $V_{gb} = 0.240eV$  and for  $V_{gb} = 0$  and their ratio. The arrows show the values of the superconducting gap  $\Delta_d = \pm 7.2meV$ , much smaller than the LDOS gap ( $\approx 24meV$ ), which is normally measured by ARPES and STM experiments.

two representative locations in the hole-rich and hole-poor phases. The hole-poor region with  $p_i = 0.021$  has a very large LDOS of  $\Delta_{PG} \approx 80K$  and  $\Delta_d = 12meV$ , as shown in the inset. At a hole-rich location ( $p(i) \approx 0.23$ ) the LDOS gap is given by  $\Delta_{PG} \approx 50meV$  with well-defined peaks at low temperature, and the superconducting gap is  $\Delta_d(T = 0) = 33meV$ . Perhaps due to the mean-field type calculations, all the gaps vanish near  $T \approx 147K$ , what can be assigned the pseudogap temperature  $T^*(p = 0.11)$ . Likewise Fig.(4) the low temperature superconducting gap  $\Delta_d$  produces small anomalies that are marked by arrows, as it was already noticed by our previous work [20] and detected experimentally by Kato et al [11, 13].

In this scenario the pseudogap phase is formed with the intragrain superconducting amplitude and the single-particle bound states. The superconducting phase also contains both the local single-particle gap  $\Delta_{PG}(i, p, T)$  and the local superconducting  $\Delta_d(i, p, T)$  but has phase coherent through the Josephson coupling among the grains. At the overdoped region  $T^*(p)$  approaches  $T_c(p)$  while their difference increases in the underdoped region. These two curves are shown in the derived phase diagram of Fig.(6). We have also plotted the EPS line  $T_{PS}(p)$  which opens all the phase separation process and it is close the observed anomaly called upper-pseudogap Timusk and Statt [1].

**Conclusions.** – The main idea of this letter is the two-body electronic attractive potential and granular structure derived from the EPS transition. We show that an effective hole-hole attraction appears from the Ginzburg-Landau free energy and the Cahn-Hilliard simulations which reveals also a microscopic granular behavior with single-particle bound states (as seen in Fig.(2)). With

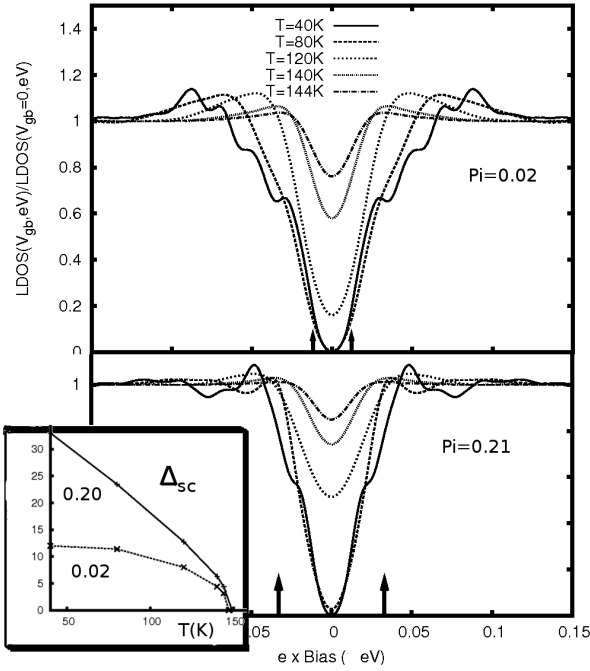


Fig. 5: The  $p = 0.11$  LDOS with  $V_{gb} = 0.44\text{eV}$ . Top panel,  $\Delta_{PG}(T)$  at a hole-poor puddle ( $p_i = 0.021$ ).  $\Delta_{PG}(T = 40\text{K}) \approx 80\text{meV}$ . The superconducting gaps  $\Delta_d(T = 40\text{K}) = 12\text{meV}$  are marked by arrows. Below, the set of LDOS curves at a hole-rich grain, ( $p_i \approx 0.20$ ) with  $\Delta_{PG}(T = 40\text{K}) \approx 50\text{meV}$  and with  $\Delta_d(T = 0) = 33\text{meV}$ . In the inset  $\Delta_d(i, T) \times T$  for each case. Both  $\Delta_{PG}(i)$  and  $\Delta_d(i)$  vanish near  $T^* = 147\text{K}$ .

the values of  $V_{gb}(p)$  that reproduced the low temperature average LDOS values of McElroy et al [8] and the values of  $T_{PS}(p)$  from the crossover or upper pseudogap line [1–3], we obtain the superconducting and pseudogap phases for all doping  $p$ . In summary:

- i*) The phase separation transition described by the Cahn-Hilliard equation minimizes the local free energy generating separated regions of different local densities.
- ii*)  $\Delta_d$  and  $\Delta_{PG}$  have completely different nature but they have the same origin, namely, the inhomogeneous potential  $V_{gb}$ . They are both present in the pseudogap and superconducting phases but distinct strength. Their differences were verified in the presence of strong applied magnetic fields and also by their distinct temperature behaviour in tunneling experiments [35].
- iii*) The LDOS are dominated by the intragrain single-particle bound states  $\Delta_{PG}$  and the superconducting gap  $\Delta_d$  produces only a small anomaly at low temperature and low bias as recently observed by some STM data [9, 11–13].
- iv*) The observed difference in the LDOS shape, called "coherent" and "zero temperature pseudogap" [8], is due to the differences in the local single-particle bound levels at hole-rich and hole-poor locations respectively.

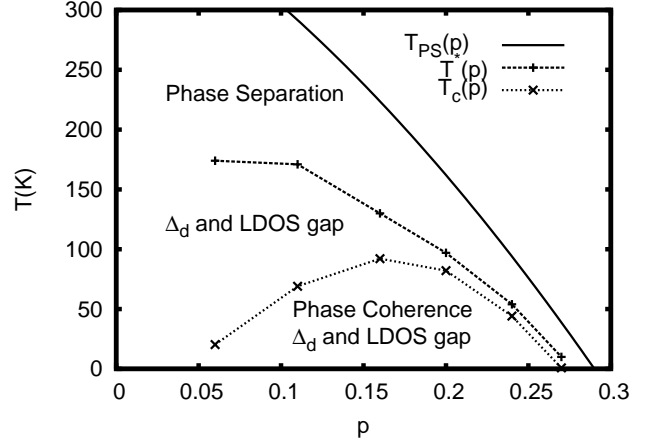


Fig. 6: The calculated phase diagram of cuprate superconductors as derived from the EPS transition  $T_{PS}(p)$  and the formation of tiny grains. The onset of single particle bound states and superconducting amplitude formation occurs at  $T^*(p)$ . The dome shape  $T_c(p)$  curve is due to Josephson coupling among the grains. These three lines are in agreement with the experimental results.

*v*) The potential barriers  $V_{gb}$  prevents phase coherence and, as in a granular superconductor, the resistivity transition occurs due to Josephson coupling among the intragrain superconducting regions (Eq.6). The  $T_c(p)$  curve is a consequence of the different behavior of  $1/R_n(p)$  which increases, and  $\Delta_d^{av}(p)$  which decreases with  $p$ .

We gratefully acknowledge partial financial aid from Brazilian agency CNPq.

## REFERENCES

- [1] TIMUSK T. and STATT B., *Rep. Prog. Phys.*, **62** (1999) 61.
- [2] TALLON J.L. and LORAM J.W., *Physica C*, **349** (2001) 53.
- [3] HUEFNER S. ET AL, *Rep. Prog. Phys*, **71** (2008) 062501.
- [4] TRANQUADA J.M. ET AL, *Nature (London)*, **375** (1995) 561.
- [5] BIANCONI A. ET AL, *Phys. Rev. Lett.*, **76** (1996) 3412.
- [6] SINGER P.M., HUNT A.W. and IMAI T., *Phys. Rev. Lett.*, **88** (2002) 47602.
- [7] S. H. PAN ET AL, *Nature*, **413** (2001) 282.
- [8] MCELROY K., ET AL, *Phys. Rev. Lett.*, **94** (2005) 197005.
- [9] GOMES KENJIRO K. ET AL, *Nature*, **447** (2007) 569.
- [10] PASUPATHY ABHAY N. ET AL, *Science*, **320** (196) 2008.
- [11] TAKUYA KATO ET AL, *J. Phys. Soc. Jpn.*, **77** (2008) 054710.
- [12] AAKASH PUSHP ET AL, *Science*, **324** (2009) 1689.
- [13] T. KATO ET AL, *J. Supercond. Nov. Magn.*, **23** (2010) 771.
- [14] RINAT OFER, AND AMIT KEREN, *Phys. Rev.*, **B80** (2009) 224521.
- [15] M. LE TACON, ET AL, *Nature Phys.*, **2** (2006) 537.
- [16] W. S. LEE, ET AL, *Nature*, **450** (2007) 81.
- [17] J. H. MA, ET AL, *Phys. Rev. Lett.*, **101** (2008) 207002.
- [18] KANIGEL A. ET AL, *Phys. Rev. Lett.*, **101** (2008) 137002.

- [19] U. CHATTERJEE, ET AL, *Nature Phys.*, **6** (2010) 99.
- [20] DE MELLO E.V.L, PASSOS C.A.C and KASAL R.B., *J. Phys.: Condens. Matter*, **21** (2009) 235701.
- [21] S. WAKIMOTO ET AL, *Phys. Rev. Lett.*, **98** (2007) 247003.
- [22] BRAY A.J. , *Adv. Phys.*, **43** (1994) 347.
- [23] SIGMUND E. and MULLER K.A (EDS., *Phase Separation in Cuprate Superconductors* (Springer-Verlag, Berlin) 1993.
- [24] CAHN J.W. and HILLIARD J.E. , *J. Chem. Phys*, **28** (1958) 258.
- [25] DE MELLO E.V.L. and SILVEIRA FILHO OTTON T. , *Physica A*, **347** (2005) 429.
- [26] DE MELLO E.V.L. and CAIXEIRO E.S., *Phys. Rev. B*, **70** (2004) 224517.
- [27] DIAS D. N. ET AL, *Physica C*, **468** (2008) 480.
- [28] DE MELLO E. V. L. and DIAS D. N., *J. Phys.C.M.* , **19** (2007) 086218.
- [29] DE MELLO E.V.L. ET AL, *Physica B*, **404** (2009) 3119.
- [30] CAIXEIRO E.S, DE MELLO E.V.L. and TROPER A.,, *Physica C*, **459** (2007) 37.
- [31] MERCHANT L. ET AL, *Phys. Rev.B*, **63** (2001) 134508.
- [32] AMBEOGAKAR V. and BARATOFF A., *Phys. Rev. Lett.* , **10** (1963) 486.
- [33] TAKAGI H. ET AL, *Phys. Rev. Lett.* , **69** (1992) 2975.
- [34] GYGI FRANÇOIS and SCHLÜTER MICHEL, *Phys. Rev. B*, **43** (1991) 7609.
- [35] KRASNOV V.M. ET AL, *Phys. Rev. Lett.*, **86** (2001) 2657.